Glucosylceramide biosynthesis is involved in Golgi morphology and protein secretion in plant cells

Su Melser, Brigitte Batailler, Martine Peypelut, Christel Poujol, Yannick Bellec, Valérie Wattelet-Boyer, Lilly Maneta-Peyret, Jean Denis Faure, Patrick Moreau

Traffic 2010; **11:** 479–490

doi:10.1111/j.1600-0854.2009.01030.x

Glucosylceramide Biosynthesis is Involved in Golgi Morphology and Protein Secretion in Plant Cells

Su Melser[1], Brigitte Batailler[2], Martine Peypelut[2], Christel Poujol[3], Yannick Bellec[4], Valérie Wattelet-Boyer[1], Lilly Maneta-Peyret[1], Jean-Denis Faure[4] and Patrick Moreau[1,2,*]

[1]Université V. Segalen Bordeaux 2, Laboratoire de Biogenèse Membranaire, CNRS UMR 5200, 146, rue Léo Saignat, 33076 Bordeaux Cedex, France
[2]Université V. Segalen Bordeaux 2, Plant Imaging Platform of BIC (Bordeaux Imaging Center), INRA Bordeaux Aquitaine BP81, 71 Avenue Edouard Bourlaux, 33883 Villenave d'Ornon Cedex, France
[3]Université V. Segalen Bordeaux 2, Photonic Imaging Platform of BIC (Bordeaux Imaging Center), Institut des Neurosciences François Magendie, Université V. Segalen Bordeaux 2, 33077 Bordeaux Cedex, France
[4]Laboratoire Biologie Cellulaire, INRA, 78000 Versailles Cedex, France
**Corresponding author: Dr Patrick Moreau, pmoreau@biomemb.u-bordeaux2.fr*

Received 9 June 2009, revised and accepted for publication 16 December 2009, uncorrected manuscript published online 17 December 2009, published online 8 January 2010

Lipids have an established role as structural components of membranes or as signalling molecules, but their role as molecular actors in protein secretion is less clear. The complex sphingolipid glucosylceramide (GlcCer) is enriched in the plasma membrane and lipid microdomains of plant cells, but compared to animal and yeast cells, little is known about the role of GlcCer in plant physiology. We have investigated the influence of GlcCer biosynthesis by glucosylceramide synthase (GCS) on the efficiency of protein transport through the plant secretory pathway and on the maintenance of normal Golgi structure. We determined that GlcCer is synthesized at the beginning of the plant secretory pathway [mainly endoplasmic reticulum (ER)] and that D,L-threo-1-phenyl-2-decanoyl amino-3-morpholino-propanol (PDMP) is a potent inhibitor of plant GCS activity *in vitro* and *in vivo*. By an *in vivo* confocal microscopy approach in tobacco leaves infiltrated with PDMP, we showed that the decrease in GlcCer biosynthesis disturbed the transport of soluble and membrane secretory proteins to the cell surface, as these proteins were partly retained intracellularly in the ER and/or Golgi. Electron microscopic observations of *Arabidopsis thaliana* root cells after high-pressure freezing and freeze substitution evidenced strong morphological changes in the Golgi bodies, pointing to a link between decreased protein secretion and perturbations of Golgi structure following inhibition of GlcCer biosynthesis in plant cells.

Key words: endoplasmic reticulum, glucosylceramide, Golgi bodies, plant cells, protein transport, secretion

Plant endomembranes contain two distinct classes of sphingolipids, glycosylated inositolphosphorylceramides (GIPCs) and glucosylceramides (GlcCers) (1,2), that are enriched in detergent-resistant membranes (DRMs) (3–5). As in other eukaryotes, the first step of sphingolipid biosynthesis in plants is catalysed by serine palmitoyltransferase (SPT), a heteromeric protein complex consisting of LCB1/LCB2 subunits (6). The essential functions of sphingolipids in plant tissues have been shown by the downregulation of LCB1 or LCB2 subunit in *Arabidopsis*, which results in a severe reduction in plant growth (6). Indeed, sphingolipid biosynthesis is essential throughout multiple stages of plant development, as shown by the defects in gametophyte development in *Atlcb2* mutants (7).

We have recently determined the intracellular distribution of lipid microdomains in *Allium porrum* seedlings by preparing DRMs from endoplasmic reticulum (ER-), Golgi- and plasma membrane-enriched fractions, and probed the involvement of sterols in their formation by treating plants with fenpropimorph (Fen), an inhibitor of cycloeucalenol cyclopropyl isomerase (CPI1) in the sterol biosynthetic pathway (8,9). Whereas most DRMs were normally isolated from the plasma membrane (PM) in control plants, they were found more abundant in the Golgi of Fen-treated plants (5). Treatment with Fen triggered a drastic shift in detergent resistance towards the Golgi membranes versus PMs, which reflected a redistribution of lipid microdomains in the secretory pathway upon a reduction in sterol biosynthesis. Another observation was that h16:0-GlcCer accumulated in Golgi DRMs after treatment with Fen, indicating that together with sterols, some GlcCer species may also be critical for membrane trafficking (5). It was shown that modification of VLCFAs (Very Long Chain Fatty Acids) altered membrane trafficking in *Arabidopsis*, possibly by modifying specific sphingolipid pools (10).

An extensive fenestration of the Golgi cisternae takes place in Fen-treated *A. porrum* seedlings (9). In addition, downregulation of LCB2 in *Arabidopsis* leads to a lack of deposition of the intine layer in pollen, which is correlated with a destructuring of the ER and Golgi membranes in mutant pollen (7). Such changes in the morphology of endomembranes may affect the steady-state membrane flux to the PM.

The accumulation of sterols and GlcCer in DRMs from Golgi membranes in Fen-treated *A. porrum* plants was correlated with a decrease of the proteins PMA2 and PIP1 in the PM (5). In a similar context, an *elo3-erg6* double mutant (blocked in C26-sphingolipid and ergosterol synthesis) was found to be lethal because of a defect in the association of the H^+-ATPase Pma1p with lipid microdomains (11). Additional data indicate that C26-sphingolipids may even be more critical than ergosterol for Pma1p sorting to the yeast PM (12). Finally, it was reported that sorting of melanosomal proteins in the Golgi of mammalian cells requires glycosphingolipids (13).

These results strongly argue in favour of an active requirement of sphingolipid biosynthesis for the normal functioning of the secretory pathway in eukaryotic organisms. The lack of studies in plants addressing this issue prompted us to develop a study to determine whether the biosynthesis of GlcCer is required for successful protein transport in plant cells. Our findings show the following:

- The enzyme responsible for GlcCer biosynthesis [glucosylceramide synthase (GCS)] in *Arabidopsis thaliana* is located at the beginning of the secretory pathway, mainly the ER.
- PDMP (D, L-threo-1-phenyl-2-decanoylamino-3-morpholino-1-propanol) is a potent inhibitor of plant GlcCer biosynthesis both *in vitro* and *in vivo*.
- The inhibition of GlcCer biosynthesis by PDMP induces critical changes in the morphology of the plant Golgi bodies.
- The inhibition of GlcCer biosynthesis by PDMP leads to a partial retention of secretory proteins in the ER and Golgi membranes.
- Overexpression of protein cargo in the secretory pathway of tobacco leaf epidermal cells increases the *de novo* biosynthesis of GlcCer.

As it is the case with sterol biosynthesis (5), our data indicate that GlcCer biosynthesis contributes to the maintenance of Golgi morphology and the transport of secretory proteins through the plant secretory pathway.

Results and Discussion

GCS is located in the ER

The aim of this study was to investigate whether the GlcCer biosynthesis by GCS is required for efficient protein secretion in plant cells. The question is only justified if indeed GluCer is synthesized at the beginning of the secretory pathway. To determine the subcellular location of GCS, we cloned the *A. thaliana* cDNA coding for the GCS (At2g19880) and produced a GCS with yellow fluorescent protein (YFP) fused at its C-terminal, which we expressed in tobacco leaf epidermal cells together with Bet11-RFP, a Golgi SNARE protein. A reticulate pattern typical of the ER was found in all the cells expressing GCS-YFP, whereas no colabelling was observed with Bet11-RFP (Figure 1).The same ER location was found for the GCS alone at different levels of expression. This localization differs from the Golgi localization of the animal GCS (14). In Drosophila, GCS GlcT-1 localizes to both the Golgi and the ER (15). The targeting signal for ER localization of GlcT-1 is not clear, but the Golgi targeting signal is located at the N-terminus. We produced a GCS construct with YFP fused at its C-terminus so that the presence of a potential Golgi targeting signal would not be masked. The presence of a dilysine (KK) motif at the C-terminus of the plant GCS reinforces the notion that the plant GCS is ER localized. The localization of the plant GCS in the ER is consistent with the localization of other sphingolipid biosynthetic enzymes such as the SPT subunit LCB1, and the ceramide synthases LOH1–LOH3 within ER membranes in plant cells (6,16); and supports the conclusion that GlcCer biosynthesis by GCS takes place at the beginning of the plant secretory pathway. Because GCS is located in an early compartment of the plant secretory pathway, and involved in the biosynthesis of GlcCer found in lipid microdomains (3–5), it became

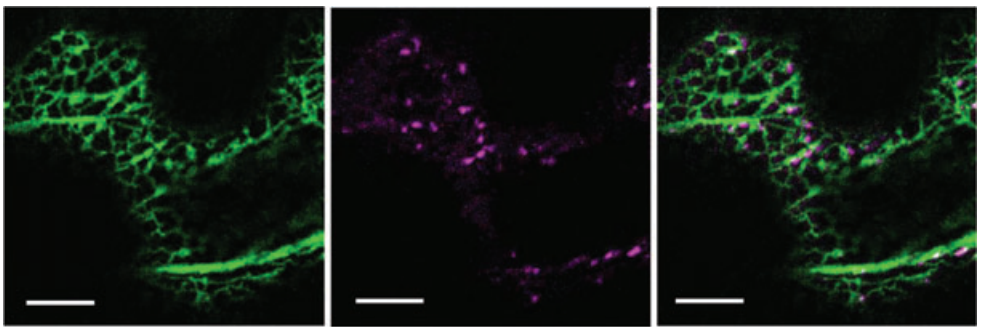

Figure 1: GCS is located in the ER. Representative expression pattern of GCS-YFP in tobacco leaf epidermal cells 48 h after cotransformation with *A. tumefaciens* carrying either GCS-YFP (green panel) or Bet11-RFP (magenta panel) expression vectors. Overlay is shown in the rightmost panel. Bars = 16 μm.

legitimate to question whether the activity of this protein was somehow related to protein trafficking.

Tobacco leaf epidermal cells as a model to study lipid impact on protein secretion

We aimed to verify and validate the suitability of tobacco leaf epidermal cells infiltrated with inhibitors as a reliable system to analyse the relation between GlcCer biosynthesis and protein transport. Recently, we showed that a reduction in the biosynthesis of sterols, induced by Fen, triggers an accumulation of lipid microdomains in Golgi membranes of *A. porrum* seedlings (5), and we took advantage of this well-known effect of Fen on the plant secretory pathway (5,9) to evaluate the protocol for inhibiting lipid synthesis in intact mature tobacco leaves. We determined that CPI1 [the main target of Fen; (8,9)] is targeted to the ER membranes of tobacco leaf epidermal cells (data not shown), as in *Arabidopsis* (17). Fen (up to 500 μM) did not disturb the biosynthesis of other lipids such as monogalactosyl diacylglycerol (MGDG; data not shown), and therefore we calculated sterol content using MGDG as a reference, to take into account the variation in the total amount of lipids between leaves and the variation between thin layer chromatography (TLC) plates. We measured the effect of Fen on sterol biosynthesis 48 h after infiltration of the drug into tobacco leaves. After lipid extraction and analysis using TLC, we determined that 50 μM and 500 μM Fen induced a dose-dependent decrease in the content of sterols in tobacco leaves (data not shown). To determine whether the tobacco leaf epidermal cells could be used to investigate the effect of lipid metabolism on protein transport, we expressed *N*-SecYFP [a secretory version of YFP; (18)] in the absence or presence of 500 μM Fen. The calculated ratio of mean fluorescence intensity at the cell surface to that of the whole cell indicated a 30% decrease in *N*-SecYFP secretion when Fen was infiltrated together with *Agrobacterium tumefaciens* carrying the secretory protein expression vector (data not shown). This decrease in *N*-SecYFP secretion to the apoplast was in agreement with the effect of Fen observed in leek and *A. thaliana* seedlings (5), and clearly indicated that tobacco leaf epidermal cells represented an appropriate model for testing the effect of GlcCer biosynthesis on protein secretion through an *in vivo* confocal microscopy approach.

PDMP inhibits specifically GlcCer biosynthesis both in vitro *and* in vivo

GCS catalyses the transfer of glucose from uridine diphosphate (UDP)-glucose to ceramide. Two main classes of compounds are used to inhibit GCS activity, either by mimicking the UDP-glucose or the ceramide. Inhibitors that mimic the UDP-glucose are represented by iminoalkylated sugar analogs such as NB-DNJ (*N*-butyldeoxynojirimycine) (19). The synthetic ceramide analogs (20) include P4 (D-threo-1-(3′,4′-ethylenedioxy)phenyl-2-palmitoylamino-3-pyrrolidino-1-propanol) and the isomers PDMP and PPMP (D,L-threo-1-phenyl-2-hexa decanoylamino-3-morpholino-1-propanol). PDMP contains n-acyl phenyl groups and a morpholine ring analogue to the ceramide fatty acyl chains and competes with ceramide on the formation of the charged transition state of the enzyme/UDP-glucose/ceramide complex (19). PDMP and its homologues are considered more specific and efficient than the glucose analogs (19), and PDMP is a strong inhibitor of the purified animal enzyme (21).

A previous study had shown that the inhibitor P4 does not affect non-human GCS enzymes in *in vitro* assays (22), and therefore we focused on testing only PDMP and PPMP.

To test the effect of the inhibitors on plant GCS activity, we developed an *in vitro* assay using tobacco leaf microsomal membranes. A typical *in vitro* assay was performed using 30 μg of microsomal protein and 8 μM UDP-glucose, without added ceramide. Such conditions provided a linear increase in the amount of GlcCer synthesized over the time of the assay. We were unable to obtain a consistent inhibitory effect on GCS activity when PPMP was used (data not shown). PDMP at 50 μM significantly decreased GlcCer biosynthesis with time (data not shown). To assess the specificity of PDMP, we measured the activity of related biosynthetic enzymes. Under our assay conditions, we were able to measure a significant synthesis of MGDG (data not shown) that could be accounted by the fact that the plastidial MGDG synthase is able to use glucose instead of galactose and that the microsomal membrane preparations still contain significant amounts of plastid envelope membranes. The assay conditions also allowed the synthesis of steryl glucoside (SG) and acylated steryl glucoside (ASG), which provided, along with MGDG, internal negative controls in our assays (data not shown). In this assay, the syntheses of MGDG, SG and ASG were not affected by PDMP, while the synthesis of GlcCer was decreased by up to 50% over time by the addition of 50 μM PDMP (data not shown). The results suggest that PDMP is a specific inhibitor of GCS *in vitro*. To test the effect of PDMP *in vivo*, tobacco leaf epidermal cells were infiltrated with 50, 100 or 150 μM PDMP and 10 μCi of labelled acetate for 48 h. Although the higher concentrations of PDMP were to some extent more efficient in decreasing the amounts of GlcCer biosynthesized in leaves, a higher percentage of cells became apoptotic above 50 μM PDMP, as measured by the dynamics of the cells observed using confocal microscopy. Therefore, infiltrations of 50 μM PDMP were used in following experiments, which induced a 70–80% reduction in *de novo* GlcCer biosynthesis, as measured by the radiolabelling of lipids over the 48-h treatment (Figure 2A). The specificity of the drug was confirmed by following the synthesis of GlcCer and other sugar-containing lipids for 8, 24, 36 or 48 h after infiltration of leaves with 50 μM PDMP. A decrease of about 30% in the content of GlcCer in leaves could already be observed 8–24 h after infiltration with PDMP ($p < 0.01$), reaching 60% after 36–48 h ($p < 0.001$) (Figure 2B). As observed *in vitro*, the content of MGDG (Figure S1C) and SG (Figure S1D) remained unaffected *in vivo*. In addition,

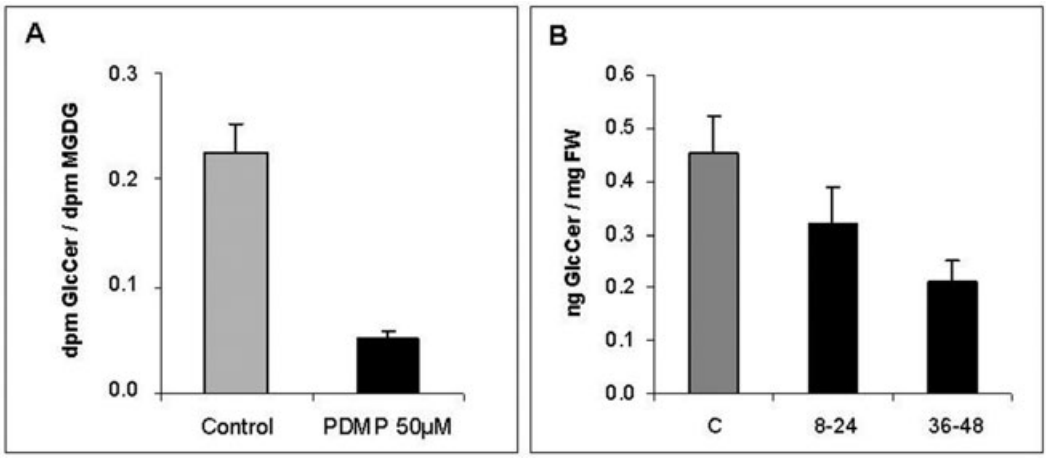

Figure 2: Inhibition of GCS activity *in vivo* by PDMP. A) *De novo* synthesis of radiolabelled GlcCer in tobacco leaves infiltrated with 10 µCi of (1-^{14}C acetate, 58 Ci/mmol) and with or without 50 µM PDMP; the controls were infiltrated with 0.5% DMSO. Lipids were extracted and analysed as described in the experimental section. The amount of labelled GlcCer was reported to that of labelled MGDG to take into account the variations of acetate incorporation between leaves. Results are means ± SD of three independent experiments. B) GlcCer content of tobacco leaves 8–24, and 36–48 h after infiltration with 50 µM PDMP, or 0.5% DMSO (control, C). GlcCer content of control leaves did not vary from 8 to 48 h and results are grouped in one column. Lipids were extracted and analysed as described in the experimental section. The content of GlcCer is expressed as nanogram per milligram of fresh leaf weight (FW), and represents the mean ± SD of three independent experiments.

we did not find any variation in the total amounts of the different phospholipids (data not shown).

Finally, we checked whether the biosynthesis of the complex sphingolipid GIPC could also be affected by treatment with PDMP. For this, the spot corresponding to GIPC was recovered from TLC plates developed using a solvent system to separate polar lipids (23), and long chain bases (LCBs) were analysed (24). HPLC analyses of the GIPC-derived LCBs showed that the trihydroxy species t18:0 and t18:1(8E) represented nearly 90% of the total LCB (Figure S1A), which is a typical composition for plant GIPC (1). LCBs derived from radiolabelled GIPC did not vary significantly upon PDMP treatment (Figure S1B), indicating that PDMP was specific to GlcCer biosynthesis.

Effect of inhibiting GlcCer biosynthesis on the morphology of the Golgi

The Golgi apparatus is considered a key protein sorting station in the secretory pathway. We found in a previous study that the inhibition of sterol biosynthesis by Fen induced a fenestration of the Golgi apparatus in leek cells (9), suggesting a prominent role for sterols in Golgi maintenance in plant cells. The association of sterols and GlcCer in membranes prompted us to examine whether the GlcCer biosynthesis was required for the maintenance of Golgi morphology. The examination of Golgi in infiltrated tobacco leaves was hindered by the difficulty to fix the extensively vacuolated epidermal cells correctly enough to allow observation of Golgi structure. Therefore, we focused on root cells from *A. thaliana* seedlings. We first confirmed that PDMP was able to inhibit GlcCer biosynthesis *in vivo* in *Arabidopsis* seedlings to a similar extent (50–60%), as it was determined for tobacco leaf epidermal cells. Ultrastructure was analysed in epidermal and cortical cells of the division zone and the beginning of the elongation zone of the root. Golgi bodies with normal cisternae organized into typical Golgi stacks were observed in the control root cells (Figure 3A). In PDMP-treated root cells, the morphology of the Golgi bodies appeared severely affected, mainly characterized by modified cisternal producing a misaligned stack, often surrounded by swollen vesicles (Figure 3B). Morphometric analyses revealed that the thickness of the stack of the Golgi bodies (*cis* to *trans* distance) was unaffected, but the cisternal thickness as well as the stack width were significantly decreased in the PDMP-treated root cells ($p < 0.01$ and $p < 0.05$, respectively) (Figure 3C). In addition, the number of vesicles/vesicular structures in the vicinity of the remaining Golgi stacks in PDMP-treated root cells was increased ($p < 0.05$). The data strongly suggest that in plant cells, the Golgi partially disaggregates into vesicular structures upon inhibition of GlcCer biosynthesis by PDMP.

Effect of inhibiting GlcCer biosynthesis on the secretion of marker proteins

To investigate the effect of GlcCer synthesis on protein secretion, we transformed tobacco leaves with *A. tumefaciens* carrying the plasmid for expression of the soluble secretory protein *N*-SecYFP or the integral membrane protein marker PMA4 [an H^+-ATPase of the PM; (25)], in the absence or presence of 50 µM PDMP. Fluorescence of protein markers was quantified using Metamorph software in 20–25 cells per condition

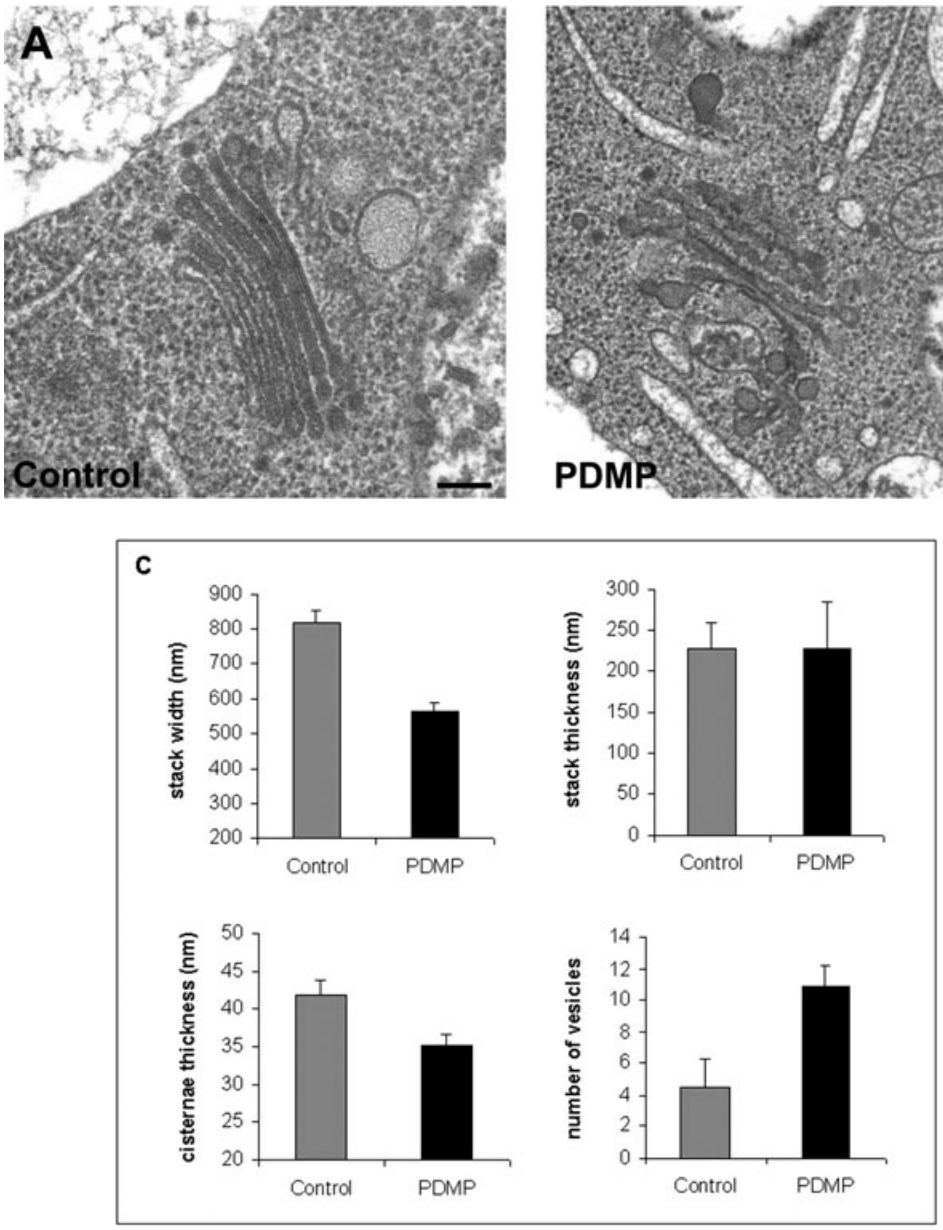

Figure 3: Effect of PDMP on Golgi morphology. Typical appearance of Golgi bodies in control *Arabidopsis* seedlings that were incubated for 48 h in culture medium (A) or treated with 10 μM PDMP in culture medium (B). Bars in (A) and (B) = 100 nm. C) Morphometric quantification of the Golgi bodies as determined with the ImageJ software.

(+ or − PDMP) per experiment, and the experiments were repeated at least four times.

Under normal conditions (in the absence of PDMP), N-SecYFP was highly secreted to the apoplast (Figure 4A), as it has been observed previously (18). In contrast, the fusion protein was partly retained in the intracellular membranes in the presence of PDMP (Figure 4B). The ratio *F*s/*F*i of mean fluorescence intensity at the cell surface (*F*s) to the mean fluorescence intensity of intracellular membranes (*F*i) shows clearly an important decrease in the presence of PDMP (Figure 4C, $p < 0.01$). In addition, the calculated ratio *F*s/*F*t of mean fluorescence intensity at the cell surface (*F*s) to the mean fluorescence intensity of the whole cell (*F*t) confirmed a 35–40% decrease in the fluorescence of *N*-SecYFP at cell surface (Figure 4C, $p < 0.01$). The decrease was accompanied by a concomitant 30–35% increase in the mean fluorescence intensity of intracellular membranes (*F*i/*F*t, Figure 4C, $p < 0.05$), indicating that the inhibition of GlcCer biosynthesis by PDMP effectively decreased the delivery of *N*-SecYFP to the cell surface.

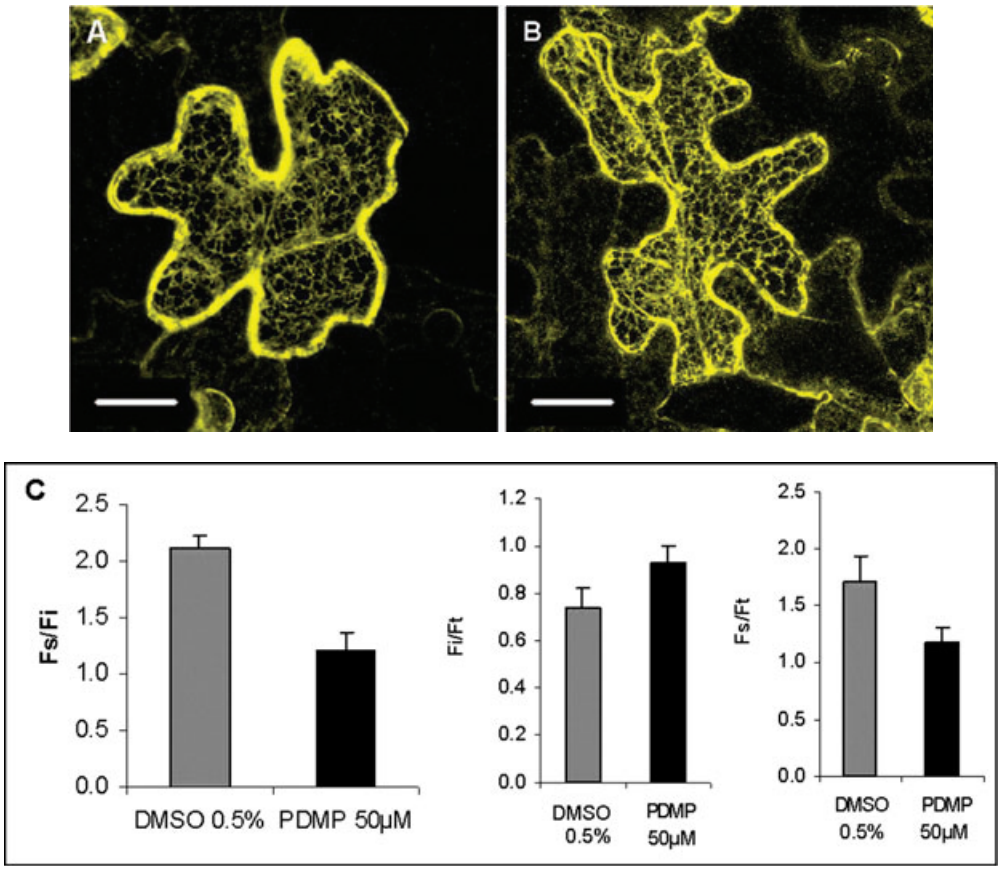

Figure 4: Effect of PDMP on *N*-SecYFP secretion to the apoplast. Representative fluorescence pattern in tobacco leaf epidermal cells 48 h after transformation with *A. tumefaciens* carrying the *N*-SecYFP expression plasmid in the (A) absence or (B) presence of 50 µM PDMP. Bars in (A) and (B) = 20 µm. C) Quantification of the mean fluorescence intensity at the cell surface Fs relative to that of the fluorescence intensity in intracellular membranes Fi (Fs/Fi) and to that of the whole cell Ft (Fs/Ft), and quantification of the mean fluorescence intensity in intracellular membranes Fi relative to that of the whole cell Ft (Fi/Ft).

We then examined the effect of GluCer synthesis on the transport of the membrane protein PMA4. When PMA4 was expressed in the absence of PDMP, the fluorescence was present only at the surface of the cell (Figure 5A), as expected for a PM marker. However, PDMP-treated cells presented, in addition to the normal PM labelling, fluorescent punctae reminiscent of Golgi bodies (Figure 5B,C). In addition, an ER-like pattern could also be observed (data not shown), although less frequently. To identify the nature of the punctate labelling in PDMP-treated PMA4 cells, we coexpressed PMA4 together with Bet11, a Golgi SNARE marker (18,26). Bet11 was chosen as a Golgi marker because it has been shown to label the *trans* Golgi network in protoplasts from *Arabidopsis* suspension-cultured cells (26), without interfering with the ER-Golgi traffic of membrane proteins (18), and also because it does not cycle between the ER and the Golgi as the K/HDEL receptor ERD2 or the animal sialyltransferase (ST) (27). Under normal expression conditions, PMA4 was found in the PM as expected, and Bet11 was found in typical dots corresponding to Golgi bodies [Figure 5D; (18)]. However, in the presence of PDMP, PMA4 colocalized with Bet11, suggesting that PMA4 was partially retained in the Golgi on its way to the PM (Figure 5E). The ratio *F*s/*F*i of mean fluorescence intensity at the cell surface (*F*s) to the mean fluorescence intensity of intracellular membranes (*F*i) shows clearly an important decrease in the presence of PDMP (Figure 5F, $p < 0.01$). The quantification of the mean fluorescence intensity of PMA4 at the cell surface (PM) compared to that of whole cells indicated a 30–35% decrease in PM mean fluorescence intensity ($p < 0.05$) and a simultaneous 25–30% increase in mean fluorescence intensity in intracellular membranes ($p < 0.05$) (Figure 5F), indicating that the inhibition of GlcCer biosynthesis reduced the transport of PMA4 to the PM. This is a similar situation as that observed in animal cells, where an absence of GlcCer led to a transport defect of membrane proteins at the Golgi (13). In a complementary approach, we performed a kinetic of expression of PMA4-GFP in the absence or presence of PDMP, and measured the amounts of the fusion protein by western blot using antibodies against PMA4 in Golgi and PM fractions prepared from the infiltrated tobacco leaves (Figure S2). Two independent

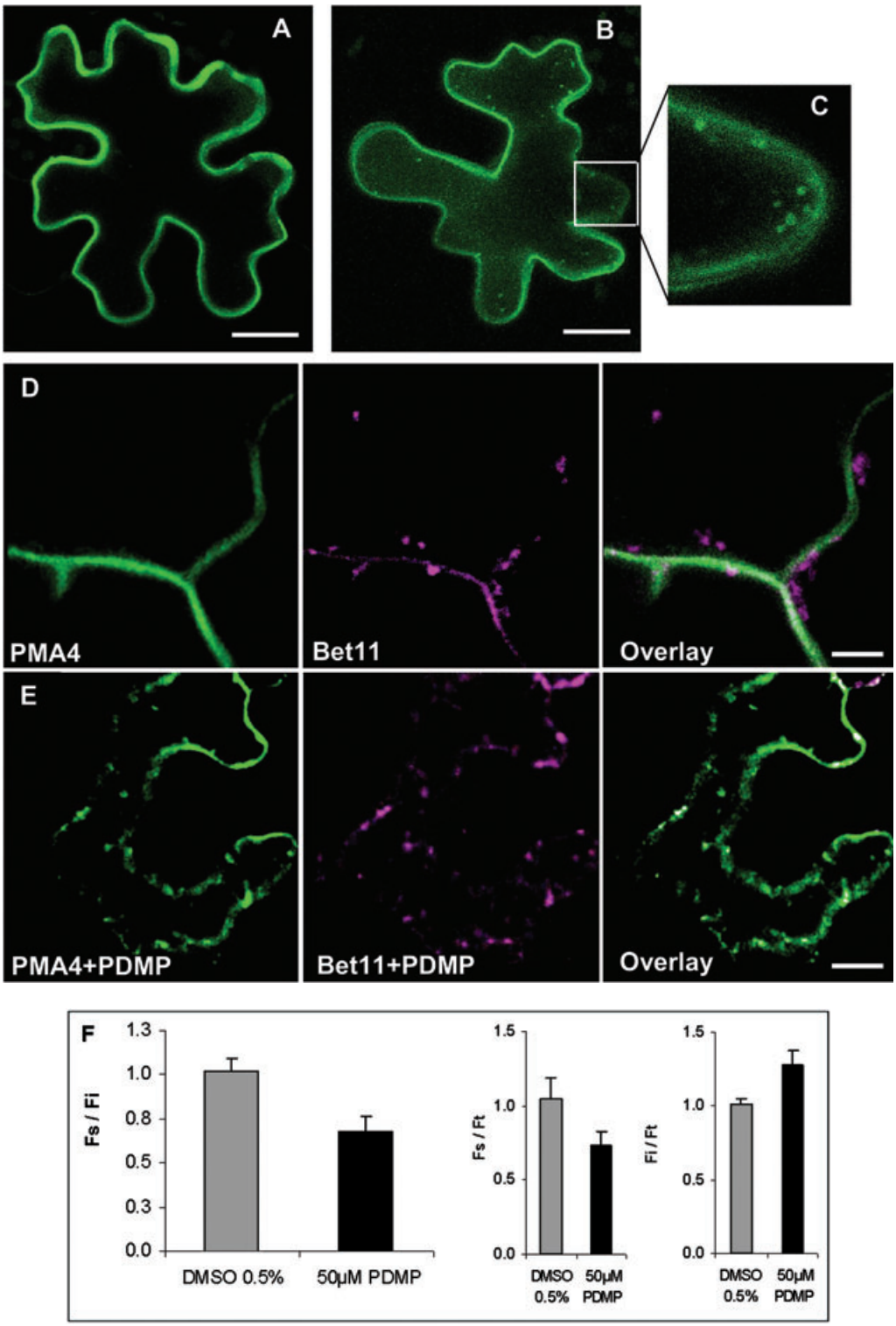

Figure 5: Effect of PDMP on PMA4 transport to the PM. Representative fluorescence patterns in (A) control cells or (B–C) PDMP-treated cells are presented. PMA4-GFP together with Bet11-RFP in tobacco leaf epidermal cells:(D) control or (E) PDMP-treated. Bars in (A) and (B) = 20 μm, bar in (D) = 5 μm and bar in (E) = 15 μm. F) Quantification of the mean fluorescence intensity at the cell surface Fs relative to that of the fluorescence intensity in intracellular membranes Fi (Fs/Fi) and to that of the whole cell Ft (Fs/Ft), and quantification of the mean fluorescence intensity in intracellular membranes Fi relative to that of the whole cell Ft (Fi/Ft).

experiments clearly confirmed that a considerable portion of fusion protein was retained in the Golgi fraction after 24 and 48 h of PDMP treatment.

In an attempt to bypass GCS, we tried to rescue GlcCer biosynthesis in PDMP-treated tobacco leaves by the addition of glucosylsphingosine as performed in Sprong et al. (13). To evaluate the feasability of such an approach in plant cells, we infiltrated tobacco leaves with PDMP, 10 μCi of labelled acetate, and with and without glucosylsphingosine for 48 h to measure *de novo* lipid synthesis. Unfortunately, we were not able to compensate the effect of PDMP on GlcCer biosynthesis by the addition of glucosylsphingosine. This result can be explained either by a low diffusion of glucosylsphingosine, which appears unlikely compared to the penetration of PDMP, or by the fact that glucosylsphingosine is not taken as a substrate in our system.

Contrary to PMA4, Bet11 did not seem affected by the PDMP treatment (Figure 5E). As ceramides and GlcCer are synthesized in the ER [(16); Figure 1], we examined the effect of PDMP on ER-to-Golgi transport with ERD2 and ST markers (18,27). Like Bet11, both markers appeared to be unaffected by PDMP under our experimental settings, using a confocal microscopy approach (Figure S3A–D).

In animal cells, transit of vesicular stomatitis virus-G (VSV-G) membrane protein from the ER to the *cis* Golgi was delayed 1.5-fold after treatment with 75 μM PDMP (28), suggesting the need for a certain level of GlcCer biosynthesis in the ER-to-Golgi transit of a membrane protein destined to the cell surface. However, unlike *N*-Sec and PMA4, ERD2 and ST were not affected in their transport to the Golgi, pointing to a lesser need for GlcCer in the ER-to-Golgi transport of proteins destined to the Golgi in plant cells, compared to proteins ultimately destined to the cell surface.

Overexpression of secretory protein cargo induces an increase in GlcCer and sterol biosynthesis

The observed intracellular retention of secretory proteins in tobacco leaf epidermal cells was positively correlated to the inhibition of GlcCer biosynthesis by PDMP. As GlcCer was necessary for the transport of proteins to the cell surface, we investigated whether an increase in the load of secretory proteins in plant cells was also accompanied by an increase in GlcCer biosynthesis. To test such a correlation, we overexpressed either the soluble secretory *N*-SecYFP or the membrane PMA4, and compared them to the overexpression of ERD2 [which does not traffic beyond the Golgi; (18,27)] and to the non-secretory cytosolic protein ranBP1 [the Ran-binding protein RanBP1a; (29)]. Lipids normally present in the membranes of the secretory pathway were analysed and quantified after radiolabelled acetate incorporation during the time of overexpression (i.e. 48 h). The results are presented in Figure 6. We did not find any increase in the amounts of phospholipids (Figure 6A), SG (Figure 6C) or free fatty acids (Figure 6E), upon overexpression of any of the four proteins tested. A significant twofold increase in the biosynthesis of GlcCer was observed when the secretory *N*-Sec and the integral membrane PMA4 proteins were overexpressed (Figure 6B). A similar increase in sterol levels was observed during *N*-Sec and PMA4 overexpression, although a lower increase could also be seen with ERD2 and RanBP1 (Figure 6D). The data strongly support the proposal that secretion of an increased load of the secretory proteins *N*-Sec and PMA4 beyond the Golgi induced a *de novo* biosynthesis of sterols and of GlcCer in particular. It has been recently shown that the *de novo* formation of ER export sites is induced by membrane cargo (30). Our results indicate that delivery of secretory proteins beyond the ER/Golgi also requires additional biosynthesis of specific lipids involved in the secretory pathway (5). Unlike *N*-Sec and PMA4, overexpression of ERD2 did not stimulate GlcCer biosynthesis in tobacco leaves (Figure 6B), again pointing to a lesser need for GlcCer in the ER-to-Golgi transport of proteins as seen in Figure S3A–D.

Altogether, our results clearly point out a requirement of GlcCer biosynthesis for post-Golgi targeting of proteins. This is in agreement with a previous study in animal cells, which was the first to show that a defect in GlcCer induced an accumulation of transported membrane proteins in the Golgi (13). RNAi suppression of the *Arabidopsis LCB2a* and *LCB2b* genes has been shown to induce strong defects in the endomembrane system of pollen (7). Disturbing the metabolism of phosphatidic acid (31) or sterols (9) also leads to critical structural modifications in the morphology of the Golgi. Several studies in various eukaryotes have similarly correlated sphingolipid and/or sterol metabolism with protein assembly, transport and endomembrane dynamics (5,7,9–13,32), and it was recently proposed that GlcCer may exert specific functions at the cytosolic surface of the ER and Golgi membranes in protein sorting and transport events in animal cells (33 and references therein). It was suggested that such functions may be strongly regulated by the glycosphingolipid transfer protein FAPP2 (33), controlling GlcCer concentration in membrane domains. Recently, the *A. thaliana* glycosphingolipid transfer protein (GLTP1) was found to regulate vesicular transport to the PM/tonoplast during root hair development (34), probably by supplying GlcCer to membrane microdomains. When placed in the context of previous reports, our data support the conclusion that GlcCer biosynthesis is essential in the maintenance of Golgi morphology, membrane dynamics and protein trafficking in plant cells.

Material and Methods

Cloning of GCS and CPI1

A cDNA clone of *A. thaliana* GCS (At2g19880) was obtained from Riken (Japan). cDNA of CPI1 (At5g50375, 43) was obtained from RNA isolated from roots and leaves of 3-week-old *A. thaliana* seedlings. RNA was purified with the RNeasy Plant Mini Kit (Qiagen) and reverse transcribed

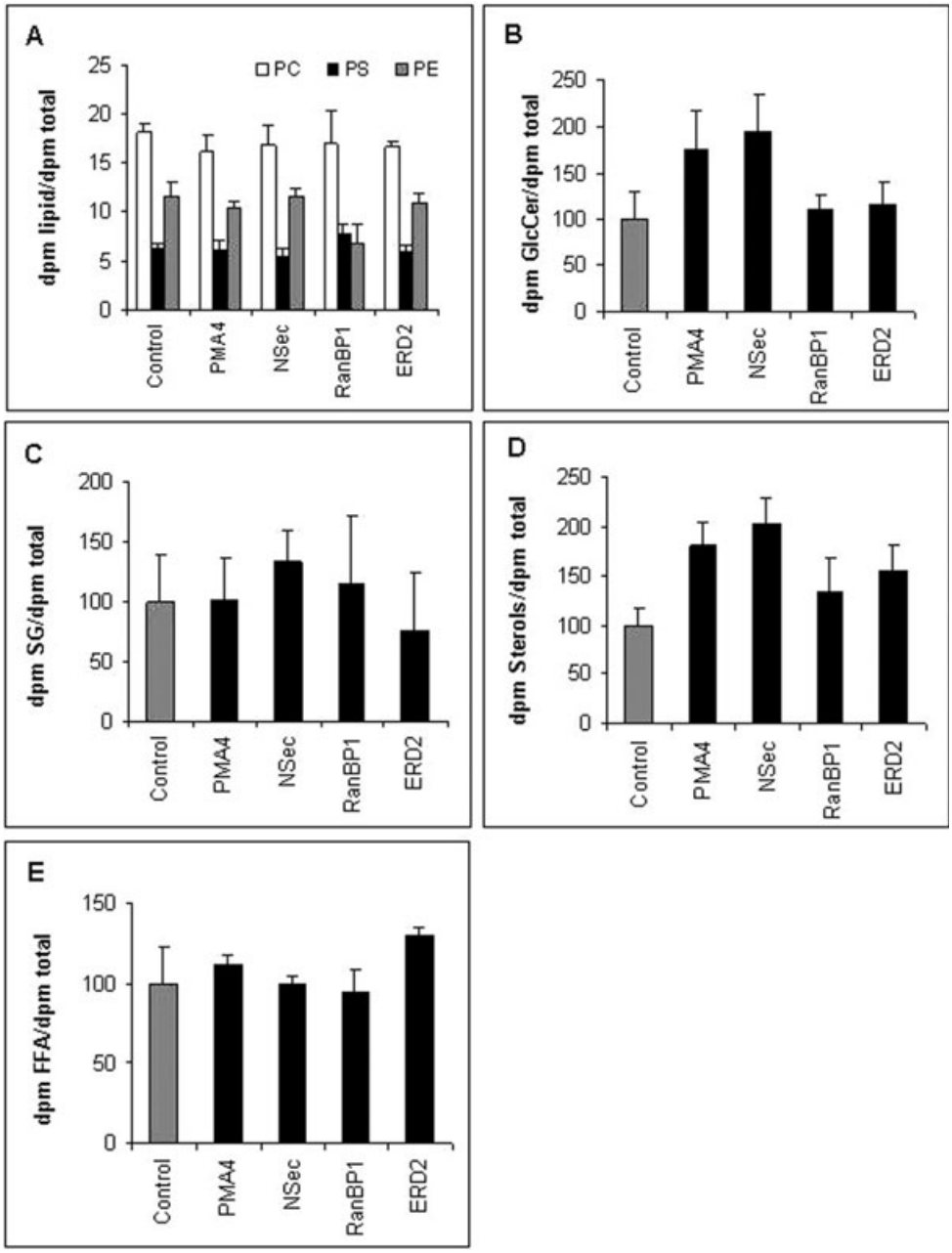

Figure 6: Overexpression of secretory proteins induces an increase in GlcCer and sterol biosynthesis. Tobacco leaf epidermal cells were incubated with radiolabelled acetate for 48 h. The acetate solution was either infiltrated alone, or with *Agrobacterium* carrying *N*-Sec, PMA4, ranBP1, or ERD2 expression constructs to examine the effect of protein overexpression on *de novo* lipid biosynthesis in the plant secretory pathway. A) Labelling in phosphatidyl choline (PC), phosphatidyl serine (PS) and phosphatidyl ethanolamine (PE). B) Labelling in GlcCer, $p < 0.01$ in control versus *N*-Sec or PMA4. C) Labelling in steryl glucoside. D) Labelling in sterols, $p < 0.01$ in control versus *N*-Sec or PMA4, $p < 0.05$ in control versus RanBP1 or ERD2. E) Labelling in free fatty acids (FFAs).

with the StrataScript First-Strand Synthesis System (Stratagene). CPI1 cDNA was amplified with the primers 5′-atg tca gga tct tct tca ccg agc ttg-3′ and 5′-tca att gga gaa cca tgg taa tcc aga ctg-3′. The polymerase chain reaction (PCR) product was purified with the QIAquick Gel Extraction Kit (Qiagen), and cloned into pGEM-T Easy (Promega) in the *Escherichia coli* TOP10F′ strain. Plasmids were then purified with the GenElute Plasmid Mini Prep Kit (Sigma), and controlled by digestion with *Eco*RI and sequencing.

Sequences of GCS and CPI1 were reamplified with specific primers to add the restriction sites *Xba*I (5′) and *Sal*I (3′) and suppress the stop codons. The PCR products were purified and cloned as described above. The resulting plasmids were digested with *Xba*I and *Sal*I, and the sequences were introduced into the expression vector pVKH18En6-YFP in which the YFP is fused to the C-terminus of the GCS or CPI1 constructs. *E. coli* DH5α strains were transformed with the expression vectors to produce the plasmids used to transform the *A. tumefaciens* strain GV3101 used in

the infiltration experiments. Additional constructs used in this study were ERD2-GFP and Bet11-RFP from Ref. (18), *N*-SecYFP from Ref. (35) and PMA4-GFP kindly provided by B. Lefebvre (25).

Plant material and transient expression systems

Four-week-old tobacco (*Nicotiana tabacum* cv. Xanthi) greenhouse plants grown at 22–24°C were used for *A. tumefaciens*-mediated transient expression (35,36). *A. tumefaciens* was cultured at 28°C, until the stationary phase (approximately 24 h), washed and resuspended in infiltration medium [50 mM MES, 0.5% (w/v) glucose, 2 mM Na_3PO_4, 100 μM acetosyringone (Aldrich) pH 5.6]. The bacterial suspension was inoculated using a 1-mL syringe without a needle by gentle pressure through a <1-mm hole punched on the lower epidermal surface (36). Transformed plants were incubated under normal growth conditions for 2 days at 22–24°C.

Confocal microscopy and fluorescence quantification

Transformed leaves were analysed 48 h after infiltration. Confocal imaging was performed using a Leica TCS SP2 confocal microscope fitted with a 63× oil immersion objective, numerical aperture (NA) 1.4. For imaging expressions of green fluorescent protein (GFP) and YFP constructs, excitation lines of an argon laser at 488 and 514 nm were used alternately with line switching using the multitrack facilities of the microscope. Imaging settings were as described (18,27,36), and postacquisition image processing was performed with the Leica LCS and ImageJ software. For fluorescence quantification, 25–30 z-sections were collected at 1.2–1.5 μm intervals using identical acquisition settings between control and treated cells and with 1 airy unit pinhole. Following acquisition, the background noise was subtracted from each image using a background Region Of Interest (ROI) and processed by applying a 5 × 5 pixel median filter to reduce high-frequency noise. Then an arithmetic projection was made of the 3D stack of images. The image was then thresholded for light objects and outline/cut tools were used to measure separately the whole cell and the section corresponding to the cell surface. Average fluorescence intensity, total fluorescence and cell area were measured for each cell using Metamorph's Integrated Morphometry Analysis (BIC platform, Université V. Segalen Bordeaux 2). No significant variation of cell area and total fluorescence per cell were observed under our experimental conditions (data not shown).

Transmission electron microscopy (TEM) and morphometric analyses

Thirteen-day-old *A. thaliana* seedlings were incubated for 48 h in liquid ½ Murashige & Skoog media (MS media) supplemented with 10 g/L sucrose. PDMP at 10 μM (PDMP-treated roots) or an equivalent volume of DMSO (control roots) was added to the media. Small root sections were flash-frozen at 2000 bars using an EM-Pact High Pressure Freezer (Leica Microsystems) and the samples were kept in liquid nitrogen. The root sections were transferred to vials containing substitution medium, consisting of 2% osmium tetraoxide in anhydrous acetone precooled to −90°C. Substitution was performed in an Automated Freeze Substitution System (Leica), with temperature increase at a rate of 4°C/h from −90°C to 0°C. Samples were rinsed with acetone and then maintained in 1% tannic acid-acetone medium. The acetone was progressively replaced by Epon resin over 48 h at room temperature and the samples were embedded in gelatine capsules, with polymerization carried out at 60°C for 24 h. Sections of 1–1.5 μm were coloured with toluidine blue to control the fixation of the samples. Ultra-thin sections (50 nm thick) were then produced and stained with 7% ethanolic uranyl acetate for 15 min, then with 1% aqueous lead citrate for 5 min.

Micrographs were taken at 80 kV on an FEI CM10 transmission electron microscope equipped with an AMT × 60 digital camera (Elexience). Morphometric analyses were performed on Golgi bodies ($n = 50$) from cortical and epidermal cells in the division/early elongation zone on three separately treated roots per treatment. Analysis was performed using ImageJ software.

Isolation of microsomal membranes from N. tabacum *leaves*

Leaves from 4–6-week-old tobacco plants (*N. tabacum* cv. Xanthi), grown in a growth chamber at 22–24°C under 16/8 h day/night conditions, were homogenized in the presence of 10 mM KH_2PO_4 (pH 8.2) with 0.5 M sorbitol, 5% (w/v) PVP40, 0.5% (w/v) BSA, 2 mM salicylhydroxamic acid and 1 mM phenylmethylsulphonyl f luoride (PMSF). After filtration, the homogenate was subjected to successive centrifugations at 1000 × ***g*** for 10 min, 10 000 × ***g*** for 15 min and 150 000 × ***g*** for 90 min. The resulting microsomal pellet was suspended in the appropriate buffer for testing GlcCer biosynthesis *in vitro*. Protein concentrations were determined according to the Bradford procedure (37) using BSA as a standard.

In vitro *enzymatic assays for GCS activity*

Tobacco microsomal membranes were resuspended with 500 μL of Tris–HCl buffer (pH 7). GCS activity was determined according to a modified protocol from Nakayama et al. (38) and Lynch et al. (39).

Microsomal membranes were incubated at 0.75 μg/mL in Tris–HCl buffer containing 2.5 mM KCl, 1 mM MgCl and 50 μM ATP, pH 7.0. The concentration of UDP-glucose [^{14}C(U)] (200 mCi/mmol) was set at 2 μM and the total concentrations of UDP-glucose were adjusted from 2 to 128 μM with non-labelled UDP-glucose. Incubations at different UDP-glucose concentrations were for 90 min at 30°C, and the incubations as a function of time used 30 μg of protein and 8 μM of UDP-glucose. Reactions were stopped by adding 2 mL of chloroform:methanol (1:1, v/v).

For measuring the effect of PDMP on GCS activity, a 10-mM stock solution of PDMP in DMSO was used, and final concentrations of DMSO of 0.5% were used in all assays. DMSO alone at this concentration (and up to 1%) did not perturb the biosynthesis of GlcCer by GCS.

In vivo *labelling of lipids in tobacco leaf epidermal cells*

Ten microcurrie of [1-^{14}C] acetate (58 Ci/mmol; Amersham) was dissolved in 500 μL of infiltration medium, and leaves were infiltrated as described earlier.

The labelled acetate solution was either infiltrated alone, with *Agrobacterium* carrying the plasmid constructs to investigate the effect of protein overexpression on *de novo* lipid biosynthesis in the plant secretory pathway, or in combination with different concentrations of PDMP to determine the effect of the drug on *de novo* lipid biosynthesis. As indicated earlier, PDMP was prepared from a stock solution in DMSO, and concentrations of DMSO not exceeding 0.5% were used in all experiments.

Lipid analyses

Lipids from microsomal membranes were extracted by chloroform:methanol (2:1, v/v) for 30 min at room temperature, and then washed 3× with 0.9% NaCl. The solvent was evaporated and lipids were dissolved in an appropriate volume of chloroform:methanol (1:1, v/v).

Lipids from tobacco leaves were extracted by propan-2-ol/hexane/water (55:20:25, v/v) as in Ref. (1). Polar lipids were analysed by HPTLC (60F254 plates, Merck), using the solvent system A: methyl acetate:n-propanol:chloroform:methanol:0.25% aqueous KCl (25:25:25:10:9, v/v) according to Ref. (23). Under these conditions, GlcCer and SG do not separate. These two lipid species were separated by HPTLC using solvent system B: chloroform:methanol (85:15, v/v) (40). For analysis of radiolabelled GIPC-derived LCBs, the origin was recovered from the HPTLC plates developed in solvent system A, hydrolysed by incubating in 4 N HCl in methanol for 16 h at 70°C. The products of hydrolysis were developed using solvent system C: chloroform:methanol:2 M NH_4OH (40:10:1, v/v) and analysed using a Storm PhosphorImager (GE Healthcare) and

ImageQuant software (Applied Biosystems). Neutral lipids were analysed by HPTLC using solvent system D: hexane:ethylether:acetic acid (90:15:2, v/v) (5). Lipids were identified by comigration with known standards and quantified by densitometric analysis (5,41) using a TLC scanner 3 (CAMAG) after primuline staining (42).

The different families of lipids had to be analysed on different HPTLC plates. To take into account any variation between plates, several known amounts of the same standards were deposited on each plate before staining and the same lipid was measured on different solvent systems.

LCB separation, derivatization and separation by HPLC were performed as described previously (24).

Acknowledgments

We thank the IFR 103 (IBVM, INRA Bordeaux) and the Bordeaux Imaging Centre (BIC), University Victor Segalen Bordeaux 2 for the confocal microscope facilities at the Plant Imaging Platform and the Photonic Imaging Platform. We also thank C. Cheniclet and V. Rouyere (Plant Imaging Platform of BIC) for their help with transmission electron microscopy (TEM). We thank J. J. Bessoule for critical reading and helpful discussions. This work was financed by University Victor Segalen Bordeaux 2, CNRS and the Conseil Régional d'Aquitaine. S. M. is the recipient of a PhD fellowship from ANR (BLAN07–1_182875), France

References

1. Markham JE, Li J, Cahoon EB, Jaworski JG. Plant sphingolipids: separation and identification of major sphingolipid classes from leaves. J Biol Chem 2006;281:22684–22694.
2. Sperling P, Heinz E. Plant sphingolipids: structural diversity, biosynthesis, first genes and functions. Biochim Biophys Acta 2003; 1632:1–15.
3. Mongrand S, Morel J, Laroche J, Claverol S, Carde JP, Hartmann MA, Bonneu M, Simon-Plas F, Lessire R, Bessoule JJ. Lipid rafts in higher plant cells: purification and characterization of TX100-insoluble micro-domains from tobacco plasma membrane. J Biol Chem 2004;279:36277–36286.
4. Borner GH, Sherrier DJ, Weimar T, Michaelson LV, Hawkins ND, Macaskill A, Napier JA, Beale MH, Lilley KS, Dupree P. Analysis of detergent-resistant membranes in Arabidopsis. Evidence for plasma membrane lipid rafts. Plant Physiol 2005;137:104–116.
5. Laloi M, Perret AM, Chatre L, Melser S, Cantrel C, Vaultier MN, Zachowski A, Bathany K, Schmitter JM, Vallet M, Lessire R, Hartmann MA, Moreau P. Insights into the role of specific lipids in the formation and delivery of lipid microdomains to the plasma membrane of plant cells. Plant Physiol 2007;143:461–472.
6. Chen M, Han G, Dietrich CR, Dunn TM, Cahoon EB. The essential nature of sphingolipids in plants as revealed by the functional identification and characterization of the Arabidopsis LCB1 subunit of serine palmitoyltransferase. Plant Cell 2006;18:3576–3593.
7. Dietrich CR, Han G, Chen M, Berg RH, Dunn TM, Cahoon EB. Loss-of-function mutations and inducible RNAi suppression of Arabidopsis LCB2 genes reveal the critical role of sphingolipids in gametophytic and sporophytic cell viability. Plant J. 2008;54:284–298.
8. Rahier A, Schmitt P, Huss B, Benveniste P, Pommer EH. Chemical structure activity relationships of the inhibition of sterol biosynthesis by N-substituted morpholines in higher plant cells. Pestic Biochem Physiol 1986;25:112–124.
9. Hartmann MA, Perret AM, Carde JP, Cassagne C, Moreau P. Inhibition of the sterol pathway in leek seedlings impairs phosphatidylserine and glucosylceramide synthesis but triggers an accumulation of triacylglycerols. Biochim Biophys Acta 2002;1583:285–296.
10. Zheng H, Rowland O, Kunst L. Disruptions of the Arabidopsis enoyl-CoA reductase gene reveal an essential role for very-long-chain fatty acid synthesis in cell expansion during plant morphogenesis. Plant cell 2005; 17:1467–1481.
11. Eisenkolb M, Zenzmaier C, Leitner E, Schneiter R. A specific structural requirement for ergosterol in long-chain fatty acid synthesis mutants important for maintaining raft domains in yeast. Mol Biol Cell 2002;13:4414–4428.
12. Gaigg B, Timischl B, Corbino L, Schneiter R. Synthesis of sphingolipids with very long chain fatty acids but not ergosterol is required for routing of newly synthesized plasma membrane ATPase to the cell surface of yeast. J Biol Chem 2005;280:22515–22522.
13. Sprong H, Degroote S, Claessens T, van Drunen J, Oorschot V, Westerink BH, Hirabayashi Y, Klumperman J, van der Sluijs P, van Meer G. Glycosphingolipids are required for sorting melanosomal proteins in the Golgi complex. J Cell Biol 2001;155:369–380.
14. Futerman AH, Pagano RE. Determination of the intracellular sites and topology of glucosylceramide synthesis in rat liver. Biochem J 1991;280:295–302.
15. Kohyama-Koganeya A, Sasamura T, Oshima E, Suzuki E, Nishihara S, Ueda R, Hirabayashi Y. Drosophila glucosylceramide synthase: a negative regulator of cell death mediated by proapoptotic factors. J Biol Chem 2004;279:35995–36002.
16. Marion J, Bach L, Bellec Y, Meyer C, Gissot L, Faure JD. Systematic analysis of protein subcellular localization and interaction using high-throughput transient transformation of Arabidopsis seedlings. Plant J 2008;56:169–179.
17. Men S, Boutté Y, Ikeda Y, Li X, Palme K, Stierhof YD, Hartmann MA, Moritz T, Grebe M. Sterol-dependent endocytosis mediates post-cytokinetic acquisition of PIN2 auxin efflux carrier polarity. Nat Cell Biol 2008;10:237–244.
18. Chatre L, Brandizzi F, Hocquellet A, Hawes C, Moreau P. Sec22 and Memb11 are v-SNAREs of the anterograde endoplasmic reticulum-Golgi pathway in tobacco leaf epidermal cells. Plant Physiol 2005;139:1244–1254.
19. Asano N. Glycosidase inhibitors: update and perspectives on practical use. Glycobiology 2003;13:93R–104R.
20. Inoguchi J, Radin NS. Preparation of the active isomer of 1-phenyl-2-decanoylamino-3-morpholino-1-propanol, inhibitor of murine glucocerebroside synthetase. J Lipid Res 1987;28:565–571.
21. Paul P, Kamisaka Y, Marks DL, Pagano RE. Purification and characterization of UDP-glucose:ceramide glucosyltransferase from rat liver Golgi membranes. J Biol Chem 1996;271:2287–2293.
22. Hillig I, Warnecke D, Heinz E. An inhibitor of glucosylceramide synthase inhibits the human enzyme, but not enzymes from other organisms. Biosci Biotechnol Biochem 2005;69:1782–1785.
23. Heape AM, Juguelin H, Boiron F, Cassagne C. Improved one dimensional thin layer chromatographic technique for polar lipids. J Chromatogr 1985;332:391–395.
24. Bach L, Michaelson LV, Haslam R, Bellec Y, Gissot L, Marion J, Da Costa M, Boutin JP, Miquel M, Tellier F, Domergue F, Markham JE, Beaudoin F, Napier JA, Faure JD. The very-long-chain hydroxy fatty acy-CoA dehydratase PASTICCINO2 is essential and limiting for plant development. Proc Natl Acad Sci U S A 2008;105:14727–14731.
25. Lefebvre B, Batoko H, Duby G, Boutry M. Targeting of a *Nicotiana plumbaginifolia* H+ - ATPase to the plasma membrane is not by default and requires cytosolic structural determinants. Plant Cell 2004;16:1772–1789.
26. Uemura T, Ueda T, Ohniwa RL, Nakano A, Takeyasu K, Sato MH. Systematic analysis of SNARE molecules in Arabidopsis: dissection of the post-Golgi network in plant cells. Cell Struct Funct 2004;29:49–65.
27. Brandizzi F, Snapp EL, Roberts AG, Lippincott-Schwartz J, Hawes C. Membrane protein transport between the endoplasmic reticulum and the Golgi in tobacco leaves is energy dependent but cytoskeleton independent: evidence from selective photobleaching. Plant Cell 2002;14:1293–1309.
28. Rosenwald AG, Machamer CE, Pagano RE. Effects of a sphingolipid synthesis inhibitor on membrane transport through the secretory pathway. Biochemistry 1992;31:3581–3590.
29. Haasen D, Köhler C, Neuhaus G, Merkle T. Nuclear export of proteins in plants: AtXPO1 is the export receptor for leucine-rich nuclear export signals in *Arabidopsis thaliana*. Plant J 1999;20: 695–705.
30. Hanton SL, Chatre L, Renna L, Matheson LA, Brandizzi F. De novo formation of plant endoplasmic reticulum export sites is

membrane cargo induced and signal mediated. Plant Physiol 2007;143:1640–1650.
31. Langhans M, Robinson DG. 1-Butanol targets the Golgi apparatus in tobacco BY-2 cells, but in a different way to brefeldin A. J Exp Bot 2007;58:3439–3447.
32. Lee MC, Hamamoto S, Schekman R. Ceramide biosynthesis is required for the formation of the oligomeric H+ - ATPase Pma1p in the yeast endoplasmic reticulum. J Biol Chem 2002;277: 22395–22401.
33. Halter D, Neumann S, van Dijk SM, Wolthoorn J, de Mazière AM, Vieira OV, Mattjus P, Klumperman J, van Meer G, Sprong H. Pre- and post-Golgi translocation of glucosylceramide in glycosphingolipid synthesis. J Cell Biol 2007;179:101–115.
34. West G, Viitanen L, Alm C, Mattjus P, Salminen TA, Edqvist J. Identification of a glycosphingolipid transfer protein GLTP1 in *Arabidopsis thaliana*. FEBS J 2008;275:3421–3437.
35. Batoko H, Zheng HQ, Hawes C, Moore I. A rab1 GTPase is required for transport between the endoplasmic reticulum and golgi apparatus and for normal golgi movement in plants. Plant Cell 2000;12:2201–2218.
36. Brandizzi F, Frangne N, Marc-Martin S, Hawes C, Neuhaus JM, Paris N. The destination for single-pass membrane proteins is influenced markedly by the length of the hydrophobic domain. Plant Cell 2002; 14:1077–1092.
37. Bradford MM. A rapid and sensitive method for the quantitation of microgram quantities of protein utilizing the principle of protein-dye binding. Anal Biochem 1986;72:248–254.
38. Nakayama M, Kojima M, Ohnishi M, Ito S. Enzymatic formation of plant cerebroside: properties of UDP-glucose: ceramide glucosyltransferase in radish seedlings. Biosci Biotechnol Biochem 1995;59:1882–1886.
39. Lynch DV, Criss AK, Lahoczky JL, Bui VT. Ceramide glucosylation in bean hypocotyls microsomes: evidence that steryl glucoside serves as glucose donor. Arch Biochem Biosphys 1997; 340:311–316.
40. Hillig I, Leipelt M, Ott C, Zahringer U, Warnecke D, Heinz E. Formation of glucosylceramide and sterol glucoside by a UDP-glucose-dependent glucosyl-ceramide synthase from cotton expressed in Pichia pastoris. FEBS Lett 2003;553:365–369.
41. Macala LJ, Yo RK, Ando S. Analysis of brain lipids by high performance TLC and densitometry. J Lipid Res 1983;24: 1243–1250.
42. Van Echten-Deckert G. Sphingolipid extraction and analysis by thin-layer chromatography. Meth Enzymol. 2000;312:64–79.
43. Lovato MA, Hart EA, Segura MJ, Giner JL, Matsuda SP. Functional cloning of an *Arabidopsis thaliana* cDNA encoding cycloeucalenol cycloisomerase.J Biol Chem 2000; 275:13394–13397.

Supporting Information

Additional Supporting Information may be found in the online version of this article:

Figure S1: PDMP does not affect the amounts of GIPC, MGDG and SG *in vivo*. Tobacco leaves were infiltrated with 50 μM PDMP or 0.5% DMSO (control C). Lipids were extracted and analysed as described in the experimental section. A) LCB composition of GIPC from control and PDMP-treated tobacco leaves. B) Content of labelled GIPC-derived LCB in control and PDMP-treated tobacco leaves. Results in (A) are representative of three independent experiments combined, verified by HPTLC (not shown). Results in (B) are the mean ± SD of three independent experiments. The content of (C) MGDG and (D) SG were expressed as nanogram per milligram of fresh leaf weight (FW), and are means ± SD of three independent experiments.

Figure S2: Effect of PDMP on PMA4-GFP amounts in Golgi and PM fractions as a function of time. Kinetics (0, 24 and 48 h) of expression of PMA4-GFP in the absence or presence of PDMP was realized. The amounts of the fusion proteins PMA4-GFP were estimated on western blots using antibodies against PMA4 (25) in Golgi (GA) and PM fractions prepared from the infiltrated tobacco leaves as indicated (5). The results of two independent kinetics are shown. PMA proteins in the PM fraction from one experiment are also shown as well as the SNARE membrin 11 in the Golgi fraction from the same experiment (revealed by a specific antibody from the lab; Moreau et al., unpublished), showing that equivalent amounts of proteins had been loaded for all fractions.

Figure S3: Effect of PDMP on the delivery of ERD2 and ST to the Golgi. Tobacco leaf epidermal cells 48 h after transformation with *A. tumefaciens* carrying ERD2 or ST alone or in combination with 50 μM PDMP. Bars = 10 μm.

Please note: Wiley-Blackwell are not responsible for the content or functionality of any supporting materials supplied by the authors. Any queries (other than missing material) should be directed to the corresponding author for the article.